BCSJ

C-Ion- and X-ray-Induced Sucrose Radicals Investigated by CW EPR and 9 GHz EPR Imaging

Kouichi Nakagawa,*[1] Hideyuki Hara,[2] and Ken-ichiro Matsumoto[3]

[1]Division of Regional Innovation, Graduate School of Health Sciences, Hirosaki University, 66-1 Hon-cho, Hirosaki, Aomori 036-8564

[2]Bruker BioSpin K. K., 3-9 Moriya-cho, Kanagawa-ku, Yokohama, Kanagawa 221-0022

[3]Quantitative RedOx Sensing Team, Department of Basic Medical Sciences for Radiation Damages, National Institute of Radiological Sciences, National Institutes for Quantum and Radiological Science and Technology, 4-9-1 Anagawa, Chiba 263-8555

E-mail: nakagawa@hirosaki-u.ac.jp

Received: August 17, 2016; Accepted: September 29, 2016; Web Released: December 8, 2016

Kouichi Nakagawa
Kouichi Nakagawa received Ph.D. degree in Chemistry in January of 1989. After three years postdoctoral research associate in the Department of Chemistry at Northwestern University and University of Denver, he became Assistant Professor at Fukushima Medical University in 1992. Then, he promoted to Professor of Radiological Sciences at Hirosaki University in December of 2010.

Abstract

We investigated stable radical distribution and particle tracks in sucrose irradiated by C-ion irradiation with continuous wave (CW) electron paramagnetic resonance (EPR) and 9 GHz EPR imaging. Both EPR results were compared with X-ray irradiation at a similar dose. Radical distribution in sucrose crystals induced by C-ion and X-ray irradiation were completely different. The 2D EPR imaging results suggested that radical species were mostly located inside the sucrose crystal. Fewer radicals were found on the surface region of the sucrose crystal. The high radical intensities in relation to the C-ion energy deposition are clearly observed at Bragg peak region. No trace of the stable radicals was found after the peak region. The stable radicals of sucrose were distributed as a result of recombination of radicals induced by particle interaction. For the first time, the present EPR images showed the stable radical distribution and particle tracks in the crystal in association with particle-sucrose interaction.

1. Introduction

Sugar (sucrose) is a universal sweetener. Various foods and dry fruits contain sucrose. It is known that powdering as well as irradiating sugar produce radicals.[1] When sucrose is irradiated, some bonds in sucrose are lost and become partially bonded radicals undergoing recombination processes. Over time, the radicals became stable radicals and stay at similar intensities.[2,3] Thus, sucrose radicals have long life (stable radicals) at room temperature if no moisture is present.

Sugar grain crystal morphology is an important factor to estimate granulated sugar quality and storage stability.[4] EPR and simulation studies of spectra of crystalline sucrose radicals were performed by Matthys et al.[5] The multicomponent character of the EPR spectrum of X-ray-irradiated sucrose was suggested. They pointed out that the radical sites were carbon-centered radicals.

Understanding the effects of radiation on various materials is very important for providing information about decomposition/recombination due to radiation–material interaction. Especially, the effects caused by heavy ion particles are of special interest. Heavy ion radiation of sucrose under the same linear energy transfer (LET) and dose produces a large number of stable radicals. This was further studied by changing the LET and irradiation dose for different particles.[6,7] Recently, Nakagawa and co-workers reviewed heavy ion induced sucrose radicals.[8] In previous sucrose research, they were able to measure the existence and concentration of radicals in irradiated samples but could not identify the part of the sample from which the signal came using CW EPR.[2,3,6–8] Therefore, there remain many questions in relation to sucrose and heavy ion interaction such as radical distribution and particle tracks.

Neither distribution of the radicals nor the particle tracks could be determined by CW EPR. A new approach, 9 GHz EPR imaging, was performed to determine the radical distribution in the irradiated sample by applying a magnetic field

© 2017 The Chemical Society of Japan

gradient. Furthermore, EPR imaging can be used to find details of stable radicals produced by the interaction of particle beam and sucrose crystals.

In this report, we used EPR imaging to determine the particle tracks and the distribution of radicals induced by C-ion. The sucrose crystals were irradiated from two different directions to produce sucrose radicals in order to trap the C-ion in the crystal. Using EPR imaging, the radical distribution induced by C-ion and X-ray were compared. In addition, we analyzed particle range as well as the radical distribution in sucrose.

2. Experimental

Samples. Commercially available sucrose single crystals were purchased from Nishin Seitou Co. Ltd. Tokyo, Japan. The crystals are monoclinic with space group $P2_1$ and have two molecules per unit cell.[4] The crystals were pasted onto an EPR rod for CW EPR and EPR imaging measurements. The size of the crystals was approximately 2 mm × 3 mm × 5 mm to fit the EPR cavity. Note that further in the text sucrose crystals are simply called sucrose.

Irradiation of Samples. Schematic illustration of sucrose and two-irradiation directions are presented in Figure 1. The arrows indicate radiation direction. Approximate crystal sizes are also indicated. Schematics of the experimental setup for C-ion irradiation of sucrose is also indicated in Figure 2. Irradiation using C-ion beams was performed in a biology experiment room of the C-ion Medical Accelerator in Chiba (HIMAC) at the National Institute of Radiological Sciences (NIRS). The

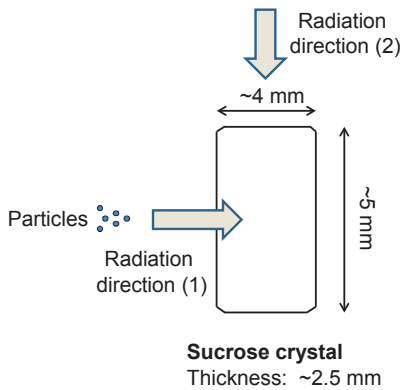

Figure 1. Schematic illustration of a sucrose crystal (space group $P2_1$) for C-ion and X-ray irradiation is presented. The arrows indicate two-radiation directions: (1) and (2). Approximate crystal size is also indicated.

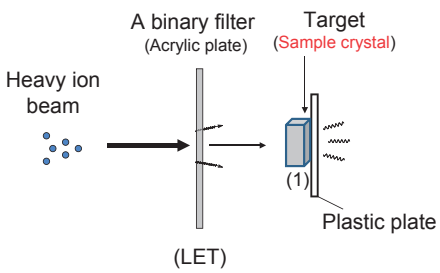

Figure 2. Schematics of the experimental setup for C-ion irradiation of the samples is presented. The acrylic plate was used to adjust the LET. Sucrose crystals were inserted in an EPR tube.

biology room was equipped with an irradiation system similar to that found in a treatment room, including dose monitors, a binary filter, and a wobbler system.[9] A target in the atmosphere was placed at a distance of 50 cm from a thin aluminum window that sealed the vacuum in the beam ducts. The wobbler system realized a 10 cm diameter uniform field with a uniformity of 2% or less. The beam intensity was measured using dose monitors installed in the beam course. A binary filter composed of poly(methyl methacrylate) plates with thicknesses ranging from 0.5 to 128 mm was used to adjust the LET.[9] The radiation dose was maintained at 50 Gy at the sample, unless otherwise noted. A schematic illustration of the experimental setting for C ion irradiation of sucrose is presented in Figure 3. EPR measurements were performed after a couple days of irradiation because our laboratory locates in the north-end of Main Island.

In addition to C-ion irradiation, X-rays (200 kV, 20 mA) were used. The dose rate was 1.23 Gy/min, and 0.5 mm copper and 0.5 mm aluminum were used to filter the low energy radiation.[10,11] All irradiated samples were maintained at ambient temperature for a few days prior to the EPR measurements.

CW EPR Settings. A commercially available JEOL RE-3X 9 GHz EPR spectrometer was used. The sample crystal was mounted as shown in Figure 3a. All CW EPR spectra were obtained with a single scan. Typical CW EPR settings were as follows: microwave power, 5 mW; time constant, 0.1 s; sweep time, 4 min; magnetic field modulation, 0.16 mT; and sweep width, 10 mT. All measurements were performed at ambient temperature.

EPR Imaging Settings. Images were acquired at room temperature on a Bruker E500 ELESYS system (Bruker BioSpin Gmbh, Karlsruhe, Germany) equipped with a high sensitivity TM resonator (10 mm diameter, Bruker). The system was operated in X-band mode at ~9.6 GHz, 100 kHz modulation frequency. For imaging, the system was equipped with water-cooled gradients allowing a magnetic field gradient up to 20 mT/cm along the X-, and Y-axes.

Sucrose (average weight ~0.0510 g) was pasted side by side onto an EPR rod (outer diameter (o.d.) ~4.0 mm) for imaging measurements as shown in Figure 3b. The rod was positioned in the center of the microwave cavity. For each measurement, the microwave power was selected within the linear section of the power intensity curve. Amplitude modulation values were chosen in such a way that they did not induce any signal

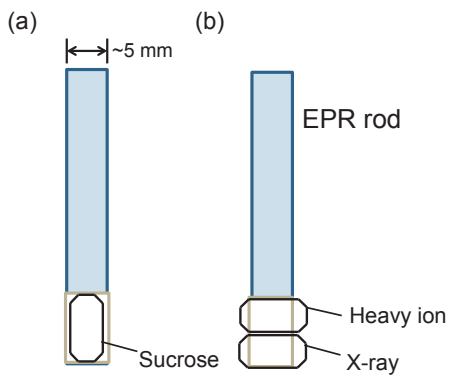

Figure 3. Schematic illustration of EPR setup for the crystal measurements is presented. Two settings (a) and (b) were used.

© 2017 The Chemical Society of Japan

Table 1. EPR imaging data acquisition conditions for the sucrose crystals

Acquisition condition	Values
Field of view/mm	6
Pixel size/mm	0.15
Gradient strength/mT cm^{-1}	12.5
Sweep time/sec	90
Total acquisition time/min	50
Modulation amplitude/mT	0.5
Microwave power/mW	2

distortion, and were always limited to the linewidth value. The conversion time, time constant, field sweep, for images, and gradient intensity of images are optimized for each sample and are given in Table 1.

Two-dimensional (2D) images were reconstructed from a complete projection set, which were collected as a function of the magnetic field gradient, using the backprojection algorithm provided in the Xepr® software package from Bruker. Before reconstruction, each projection was deconvolved using fast Fourier transformation with the measured zero-gradient spectrum to improve the image resolution. To reduce noise amplification and avoid possible division by zero at high frequencies, a low pass filter was used. The deconvolution parameters, including the maximum cut-off frequency and the width of the window in the Fourier space, were set up after viewing the shape of all projection. Spectral deconvolution and filtered backprojection were performed using the Xepr software package.

The typical EPR imaging settings were as follows: microwave power, 2 mW; time constant, 1 s; total acquisition time, 50 min; magnetic field modulation, 0.5 mT; sweep width, 15 mT; field of view, 6 mm; pixel size, 0.15 mm; and gradient strength, 5–12.5 mT/cm. The detailed acquisition parameters for sucrose are listed in Table 1. All measurements were performed at ambient temperature.

3. Results

CW EPR. Figure 4 shows EPR spectra of X-ray- and C-ion-irradiated sucrose. EPR spectra of X-ray-irradiated sucrose (top), C-ion at LET 50, 94 Gy, direction (1) (middle), and C-ion at LET 50, 94 Gy, direction (2) (bottom) are presented. EPR spectral intensities for X-ray-irradiated sucrose were stronger than those for C-ion-irradiated sucrose. In addition, slightly different EPR line-shapes were observed for C-ion-irradiated sucrose as shown in Figure 4.

EPR Imaging. Figure 5 shows EPR imaging of sucrose irradiated with C-ion and X-ray. Both crystal sizes were similar. The sucrose radicals irradiated by C-ion at LET 50, 94 Gy (top), and X-ray at 60 Gy (bottom) showed completely different images. The high color intensity is directly proportional to the radical concentration induced by C-ion irradiation. Although only half of the crystal has radical related color for C-ion irradiation, the crystal for X-ray irradiation showed the whole crystal was colored. The results indicate that C-ion impact very differently to produce free radicals. It is noted that the red color

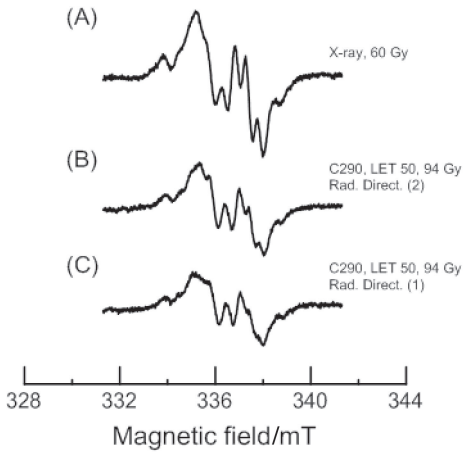

Figure 4. EPR spectra of sucrose irradiated by X-ray (top), by C-ion at LET 50, 94 Gy, radiation direction (1) (middle), and by C-ion at LET 50, 94 Gy, radiation direction (2) (bottom) are presented.

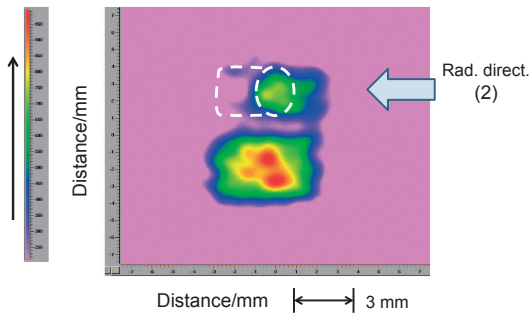

Figure 5. EPR imaging of two sucrose crystals irradiated by C-ion at LET 50, 94 Gy (top), and X-ray at 60 Gy (bottom) is shown. The arrow indicates radiation direction for C-ion. Both crystal sizes were similar sizes. The dashed circle indicates the intense color region in the middle of the crystal.

for X-ray irradiation can be characteristic of the dose distribution in the crystal.

Figure 6 shows EPR imaging of sucrose irradiated with C-ion and X-ray. EPR imaging of sucrose radicals irradiated by C-ion at LET 50, 94 Gy (top), and X-ray at 60 Gy (bottom). The radiation direction (2) was used for the crystals. Both crystal sizes were similar. The arrow indicates radiation direction for C-ion. Both crystals showed color. The intensity of color for the X-ray-irradiated sucrose was stronger than that resulting from C-ion irradiation.

Figure 7 shows EPR imaging of sucrose irradiated with C-ion. Two layers of the crystals were used for the irradiation. The second crystal showed a half of it was colored. This is the very clear results of C-ion-irradiation of sucrose. The C-ion disappeared around the middle area of the crystals.

4. Discussion

CW EPR and EPR imaging are noninvasive techniques used for the detection of unpaired electrons and have been applied to study free radicals in various materials.[12–14] Although EPR spectra of the irradiated sucrose show multiple lines (e.g. Figure 4), the peak-to-peak linewidth (ΔH_{pp}) at around the

© 2017 The Chemical Society of Japan

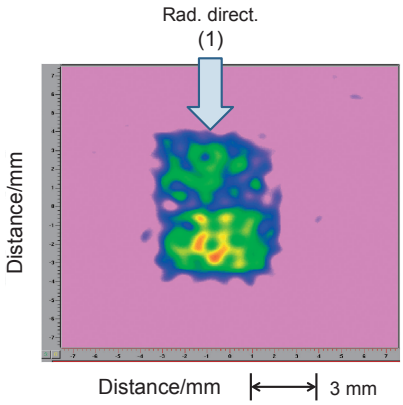

Figure 6. EPR image of two sucrose crystals irradiated by C-ion at LET 50, 94 Gy, radiation direction (1) (top) and by X-ray (bottom) is presented. Two crystals were pasted on an EPR rod side by side.

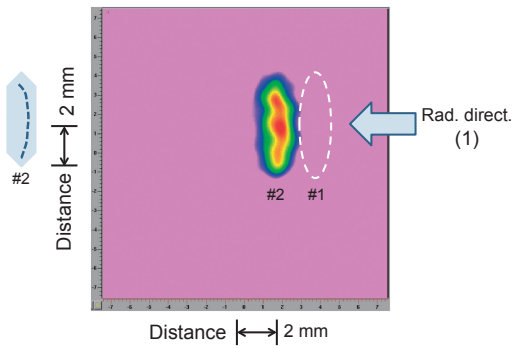

Figure 7. EPR imaging of sucrose radicals irradiated by C-ion at LET 50, 94 Gy is shown. The arrow indicates radiation direction (1). The schematic depiction of the radical distribution indicated the left-hand side of the figure. The dashed line indicates the first crystal position.

center is approximately 0.32 mT. The resolution of the images is approximately 320 µm.

Figure 5 indicates that EPR imaging of sucrose irradiated by C-ion showed intense radical concentration at approximately 2.5 mm of the crystal. EPR images of sucrose radical indicated that the irradiated crystal had a more intense color in the middle as shown in Figure 5 (the dashed circle). The dashed circle in the figure corresponds to the so-called Bragg peak. The Bragg peak can be characterized by the highest particle energy loss in a medium. The results show that EPR images corresponding to the high radical intensities in relation to the C-ion energy deposition were clearly observed. In addition, there are traces of particles as weaker signals (light green color) toward the intense region. The traces are related to stable radicals generated by C-ion. No trace of the particle track in the sucrose after the Bragg area was observed. Radical distribution in sucrose induced by C-ion and X-ray irradiation were completely different. In the case of X-ray irradiation sucrose radicals were almost uniformly distributed throughout the crystals (the lower image in Figure 5).

EPR image of the sucrose irradiated by the direction of (1) (Figure 1) shows the whole crystal colored as shown in Figure 6 (top). The C-ion went through the crystal thickness and produce stable radical in the crystal.

Two sucrose crystals were stacked for C-ion irradiation. The first crystal showed the radical distribution throughout the sucrose. The dashed line indicates the first crystal position and the data is not shown in Figure 7. Sucrose radicals of the second one exist on the region of the second crystal where particles stopped as shown in Figure 7. The red color region indicates that C-ion released their energies and disappeared in the second sucrose. It is noted that the curved shape of the color region is due to the crystal edges. The range of C-ion at LET 50, 94 Gy can be approximately 2.5 mm in sucrose. Although the red color is not uniform, the red color is indication of high radical concentration in the crystal.

5. Conclusion

The present EPR and EPR imaging investigation showed quantitative information regarding paramagnetic species distribution in the sucrose. Both 9 GHz EPR imaging and CW EPR can be useful for determining and analyzing the location of paramagnetic species in sucrose and other materials. Therefore, identifying particle tracks in the crystals can provide further insights into material-particle interaction.

Part of this research was supported by Research Project with Heavy-ion at NIRS-HIMAC, a Grant-in-Aid for Challenging Exploratory Research (24650247, JP15K12499) and for Scientific Research (B) (25282124) from the Japan Society for the Promotion of Science (JSPS) (K.N.), and A-step (AS262Z00876P) from Japan Science and Technology (JST) (K.N.).

References

1 T. Nakajima, T. Otsuki, *Int. J. Radiat. Appl. Instrum., Part A* **1990**, *41*, 359.
2 K. Nakagawa, T. Nishio, *Radiat. Res.* **2000**, *153*, 835.
3 K. Nakagawa, Y. Sato, *Spectrochim. Acta, Part A* **2006**, *63*, 851.
4 A. Bensouissi, B. Roge, J. Genotelle, M. Mathlouthi, *CrystEngComm* **2010**, *12*, 579.
5 G. Vanhaelewyn, J. Sadlo, F. Callens, W. Mondelaers, D. De Frenne, P. Matthys, *Appl. Radiat. Isot.* **2000**, *52*, 1221.
6 K. Nakagawa, K. Anzai, *Appl. Magn. Reson.* **2010**, *39*, 285.
7 Y. Karakirova, K. Nakagawa, N. D. Yordanov, *Radiat. Meas.* **2010**, *45*, 10.
8 K. Nakagawa, Y. Karakirova, N. D. Yordanov, *J. Radiat. Res.* **2015**, *56*, 405.
9 T. Kanai, M. Endo, S. Minohara, N. Miyahara, H. Koyama-ito, H. Tomura, N. Matsufuji, Y. Futami, A. Fukumura, T. Hiraoka, Y. Furusawa, K. Ando, M. Suzuki, F. Soga, K. Kawachi, *Int. J. Radiat. Oncol. Biol. Phys.* **1999**, *44*, 201.
10 K. Nakagawa, *Free Radic. Res.* **2014**, *48*, 679.
11 K. Nakagawa, K. Kobukai, Y. Sato, *J. Radiat. Res.* **2014**, *55*, 726.
12 K. Nakagawa, N. Ikota, K. Anzai, *Spectrochim. Acta, Part A* **2008**, *69*, 1384.
13 K. Nakagawa, B. Epel, *Spectrochim. Acta, Part A* **2014**, *131*, 342.
14 K. Nakagawa, *Free Radic. Res.* **2014**, *48*, 679.

© 2017 The Chemical Society of Japan